Properties of epitaxial (110) $BaTiO_3$ films from first principles

Zhigang Gui,* S. Prosandeev, and L. Bellaiche

Physics Department and Institute for Nanoscience and Engineering, University of Arkansas, Fayetteville, Arkansas 72701, USA

(Received 30 November 2011; revised manuscript received 7 December 2011; published 22 December 2011)

A first-principles-based effective Hamiltonian approach is used to simulate the temperature-versus-misfit strain phase diagram of epitaxial (110) $BaTiO_3$ (BTO) thin films. Unusual features are discovered that significantly differ from those found in BTO films grown along the "usual" [001] direction. Examples include the independency of the Curie temperature with compressive strain and the existence of specific monoclinic and triclinic phases near room temperature. These low-symmetry phases are associated with a rapid strain-induced rotation of the polarization and possess large piezoelectric and dielectric responses. Our atomistic technique provides an insight into these novel features, as well as other predicted phenomena.

DOI: 10.1103/PhysRevB.84.214112 PACS number(s): 77.55.fe, 71.15.−m, 77.22.Ch, 77.80.bn

I. INTRODUCTION

Ferroelectric (FE) thin films have gained a lot of attention because of their potentials in devices design, such as high-frequency capacitors and FE random-access memories.[1,2] Of many factors that can affect their properties, epitaxial strain has been the most investigated one. In particular, there have been a lot of calculations and experimental works devoted to epitaxial thin films made of the prototype $BaTiO_3$ (BTO) FE.[3–9] As a result, novel features have been reported in these nanostructures. For instance, FE thin films under short-circuitlike electrical boundary conditions (for which the depolarizing field vanishes or is rather small, as a result of a large screening of the polarization-induced surface charges) exhibit different directions for the spontaneous polarization and different resulting crystallographic phases, depending on the misfit strain arising from the substrate on top of which the film is grown.[4–6] Another example is the large sensitivity of the Curie temperature with misfit strain in BTO and in other FE films.[5,6,10]

Interestingly, all the aforementioned breakthroughs concern FE thin films that are grown along the [001] pseudocubic direction. On the other hand, studies aimed at determining and understanding the effects of the growth direction on properties of FE epitaxial films are rather scarce.[11–14] For instance, to the best of our knowledge the (fundamentally and technologically important) temperature-versus-misfit strain phase diagram has never been revealed for any FE film grown along the [110] direction, despite the fact that (110) FE films have been experimentally realized[15–17] and that this special growth direction has been recently shown to generate unusual phenomena.[18]

The general aim of this paper is to address such an issue by performing simulations on epitaxial (110) BTO films. Novel features are predicted to occur in these films. For instance, the Curie temperature, T_C, is nearly independent of compressive strain, unlike in (001) BTO films.[5,6] Moreover, an unexpected triclinic phase and three distinct monoclinic phases emerge in the temperature-versus-misfit strain diagram. Such latter phases allow (i) the polarization to easily rotate with strain, which generates large piezoelectric and dielectric responses near room temperature; and (ii) the (110) BTO film to easily switch its polarization's direction via a transition between different low-in-symmetry phases, by applying in-plane and out-of-plane electric fields. Items (i) and (ii) are promising to design miniaturized and lead-free devices.

The paper is organized as follows. Section II describes the effective Hamiltonian scheme presently used to simulate epitaxial (110) BTO films. Section III provides and analyzes our results. Finally, a summary is given in Sec. IV.

II. METHOD

We use the first-principles-based effective Hamiltonian[19] approach of Ref. 20, combined with Monte Carlo (MC) simulations. Its total internal energy, E_{tot}, possesses two degrees of freedom: (i) the local FE soft modes in unit cell i, $\{\mathbf{u}_i\}$ (which is proportional to the electric dipole centered on site i[19]); and (ii) the strain tensor (that contains both the homogeneous and inhomogeneous parts). E_{tot} includes 5 main parts:[19] the self-energy associated with the $\mathbf{u}_i$'s; the long-range dipole-dipole interactions; the short-range interactions between local FE modes; the elastic energy; and the interactions between strains and the $\mathbf{u}_i$'s. Three-dimensionally periodic $12\times12\times12$ BTO supercells (8640 atoms) are generated to get well-converged results. Two different coordinate systems are used: the "usual" (xyz) system for which the x-, y-, and z-axis lie along the [100], [010], and [001] pseudocubic directions, respectively, versus a new coordinate system ($x'y'z'$) chosen such as the x'-, y'-, and z'-axis are along the [001], [1–10], and [110] pseudocubic directions, respectively. The mimicking of finite-temperature properties of BTO films that are grown along the [110] pseudocubic direction, z', under various epitaxial strains is accomplished by imposing the following conditions for the homogeneous strain tensor (in Voigt notation): $\eta_1' = \eta_2' = (a_{sub} - a_{alat})/a_{alat} = \delta$, $\eta_6' = 0$, while η_3', η_4', and η_5' can relax. Here, the prime ($'$) is used to denote the values in the ($x'y'z'$) coordinate system. a_{sub} is the in-plane lattice constant of the substrate. As for a_{alat}, we assign it to the value of the lattice constant of cubic paraelectric BTO *bulk* interpolated to 0 K. δ is the misfit strain. We cool down the system for each selected δ from high temperature to low temperature with a 5 K temperature step and using 300 000 MC sweeps. We also use the correlation functions of Refs. 21 and 22 to compute the dielectric susceptibility and the piezoelectric coefficients. As detailed in Ref. 20, all the parameters of the presently used effective Hamiltonian are derived by performing first-principle calculations on relatively small supercells. This effective Hamiltonian has been shown to yield properties of $BaTiO_3$ and $(Ba,Sr)TiO_3$ (BST) systems that are in excellent agreement

with measurements and/or first-principles calculations.[20,23–28] Examples include Curie temperatures,[20] temperature gradient-induced polarization,[24] and electrocaloric[25] effects in BST materials, as well as the existence of two modes contributing to the THz dielectric response of BTO materials.[26,27] We also checked that the effective Hamiltonian approach of Ref. 20 correctly reproduces the different phases obtained by previous first-principles techniques[4,5] in (001) BTO films, when varying the misfit strain.

III. RESULTS

Figure 1 displays the predicted temperature-versus-misfit strain phase diagram for epitaxial (110) BTO. The investigated epitaxial strain ranges from around −3.5% to around +3.0%, in order to cover a strain window that is typically reachable in experiments. Notations similar to those defined in Refs. 4, 29, and 30 are used for the states appearing in Fig. 1. The general direction of the polarization in the (*xyz*) frame is also indicated there for each of these states. The paraelectric phase, labeled as p, occurs at high temperature for any δ, while six other phases, all being FE, can be seen in Fig. 1. They differentiate themselves by the hierarchy between the x-, y-, and z-components of the supercell average of the local mode (which is directly proportional to the spontaneous polarization) to be denoted by u_x, u_y, and u_z, respectively. They are (i) the c state, with $u_x = u_y = 0$, $u_z \neq 0$, for tensile strain at high temperature; (ii) the aa state, with $u_x = u_y \neq 0$, $u_z = 0$, which is the ground state for large compressive strain; (iii) the r_c state occurring in the tensile strain region at low temperature, and for which $u_x = -u_y \neq 0$, $u_z \neq 0$ with $u_z > u_x$; (iv) the r_{aa} phase that is the ground state for relatively small compressive strain and is characterized by $u_x = u_y \neq 0$, $u_z \neq 0$ with $u_z < u_x$; (v) the ab state, with $u_x \neq u_y > 0$ and $u_z = 0$, that happens at relatively small compressive strain below the Curie temperature, T_C; and (vi) the *abc* phase that is centered around the zero-misfit strain just below T_C. In this latter phase, u_x, u_y, and u_z, are different from each other and are finite, with u_y changing its sign from positive to negative when crossing the compressive-to-tensile border. The space groups of these phases are obtained from the use of the "FINDSYM" program[31] and are indicated in Ref. 32.

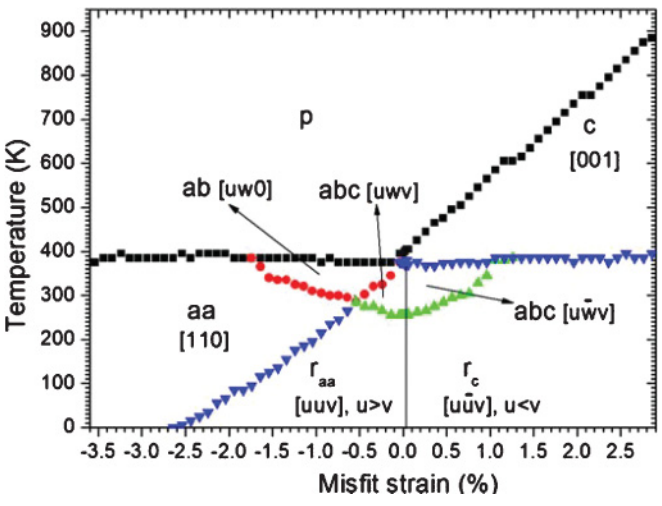

FIG. 1. (Color online) Predicted temperature-versus-misfit-strain diagram in epitaxial (110) BTO film. The direction of the polarization for each phase is indicated in the (*xyz*) coordinate frame near the phases' names.

The phase diagram shown in Fig. 1 is significantly different from that of BTO films grown along the "conventional" [001] direction.[4,5] For instance, parts of the diagram for (110) BTO films appear to have swapped from left to right (and *vice versa*) with respect to parts of the diagram for (001) films: the aa and r_{aa} phases exist for compressive strains, and the c and r_c states are in the tensile strain region in (110) BTO films, while it is exactly the opposite situation in (001) BTO films. Such swapping can be understood by the fact that compressive strain favors the formation of out-of-plane polarization while tensile strain favors in-plane components of the polarization,[4,5,29] and that the out-of-plane direction is different between (001) and (110) films.

Another major difference between (001) and (110) BTO films is that T_C is basically independent of the compressive misfit strain in these latter films: the transition temperatures from p to aa but also from p to ab occur at the same temperature of around 385 K for any δ ranging between 0.0% and −3.6%. Interestingly, 385 K is nearly our predicted T_C of BTO *bulk*,[20] which is very close to its experimental value.[33] The FE-to-FE c-to-*abc* and c-to-r_c transitions are also found to occur near 385 K, independently of the value of the *tensile* strain.

To understand these latter features, Figs. 2(a) and 2(b) show the three Cartesian components of the local modes at 5 K with respect to δ along the x, y, z directions and x', y', z' directions, respectively. Figure 2(a) reveals that the x- and y-components of the local modes stay nearly constant for any studied compressive strain (these two components are equal to each other, which also renders the out-of-plane z'-component of the polarization to be nearly independent of compressive strain). This insensitivity is correlated with the aforementioned independency of the p-to-aa and p-to-ab transition temperatures with the compressive strain (since these two transitions are characterized by the activation of x- and y-components of the polarization), as consistent with the fact that the so-called ϕ^4 model predicts that T_C is proportional to the value of the spontaneous polarization at 0 K.[34,35] Such strain insensitivity of the local modes arises mainly from a competition between various elastic-mode interactions[19] and the anharmonic part of the FE soft-mode self-energy[19] in (110) BTO films. For instance, in the aa phase, the interactions between local modes and strains $\{\eta_1, \eta_2, \eta_3\}$, as well as the soft-mode anharmonic intrasite interaction, lead to an enhancement of the x- and y-components of the local modes when increasing the magnitude of the compressive misfit strain, while the interaction between local modes and the shear strain η_6 contributes in an almost precisely opposite manner (note that the analytical expressions of these interactions are provided in Ref. 19). This competition also leads to the x- and y-components of the local mode being independent of the strain, and equal to each other in magnitude, in the tensile region (but with the sign of the y-component being now negative, in order to have an in-plane, y'-component of the polarization being strain-independent). As a result, and as consistent again with the ϕ^4 model, the c-to-*abc* and c-to-r_c transitions occur at nearly the same temperature for

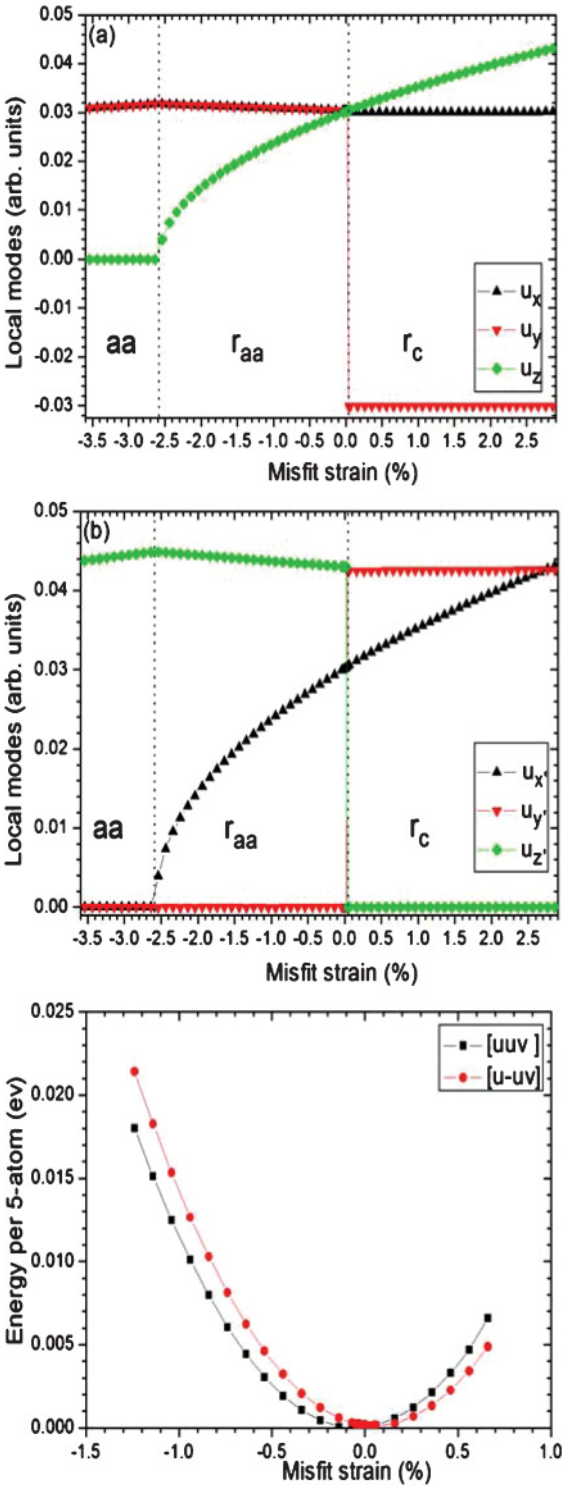

FIG. 2. (Color online) Dependency of properties with the epitaxial strain in the (110) BTO film at 5 K. Panels (a) and (b): the local modes in the (xyz) and ($x'y'z'$) coordinate frame, respectively. Panel (c): the total energy for the two stable phases having a polarization lying along [uuv] and [u–uv]. The zero in energy corresponds to the energy associated with the zero misfit strain.

any studied tensile misfit strain (since these two transitions are also accompanied by the formation of x- and y-components of the polarization).

Note also that the fact that Fig. 1 further reveals that the transition temperatures of aa-to-r_{aa}, ab-to-abc, and p-to-c strongly depend on the strain is associated with the large strain sensitivity of the z (or equivalently, x') component of the polarization depicted in Fig. 2. Such strong sensitivity occurs, because, unlike for the strain independency of the x- and y-components of the polarization, the different involved energetic terms do not cancel each other.

Figure 2 also shows that the polarization of the r_{aa} state continuously rotates from [110] to [111] as the compressive strain decreases in magnitude, therefore acquiring an increasing in-plane, x'-component in addition to a nearly strain-independent out-of-plane z'-component. Moreover, the strain-induced r_{aa}-to-r_c transition is of first order and is associated with a sudden change of the direction of the polarization from the [111] to [1–11] pseudocubic direction around $\delta = 0.0\%$. Such change of direction allows the polarization to fully lie in the epitaxial (110) plane. As the tensile strain increases, the polarization of the r_c state deviates more and more from the [1–11] direction via an increase of its z-component but remains in-plane. All these features are also found for any temperature up to 250 K, but with the value of the local modes decreasing as the temperature increases.

Moreover, Fig. 2(c) shows the total energy at 5 K versus the misfit strain (for relatively small δ) for the two stable phases associated with a polarization lying along the [uuv] and [u–uv] directions, respectively. It further confirms that a polarization along [uuv] is more energetically favorable than a polarization along [u–uv] for compressive strain (and *vice versa* for a tensile strain). This is consistent with the fact that compressive (respectively, tensile) strain favors out-of-plane (respectively, in-plane) polarization.[4,5,29] Interestingly and as confirmed by further calculations, Fig. 2(c) implies that applying a relatively small electric field along the out-of-plane direction to the r_c state for a small tensile strain will allow the (110) BTO film to reach the metastable state for which the polarization is along a [uuv] direction, leading to the appearance of the out-of-plane, z'-component of the polarization. Then applying an electric field along the in-plane, y'-direction will make the system go back to its r_c ground state, therefore vanishing the out-of-plane component of the polarization. Such field-induced scheme can lead to the design of memory devices using the occurrence and vanishing of the z'-component of the polarization. Similar strategy can be used in the compressive region but by applying first in-plane and then out-of-plane electric fields. Figure 2(c) also shows that the r_{aa} and r_c phases are degenerate for $\delta = 0.0\%$, as consistent with the fact that the polarization of the ground state of BTO bulk can be along any of the eight different possible $\langle 111 \rangle$ directions.

Direct density-functional theory[36] calculations were also performed[37] and confirmed all the aforementioned ground-state properties of (110) BTO films, namely (i) the absolute values of the x- and y-components of the polarization of the r_{aa} and r_c phases are nearly independent of the misfit strain; (ii) the strain-induced change in hierarchy between the two total energy curves depicted in Fig. 2(c), therefore further demonstrating the first-order transition between the r_{aa} and r_c phases; and (iii) the degeneracy of the r_{aa} and r_c phases at $\delta = 0.0\%$.

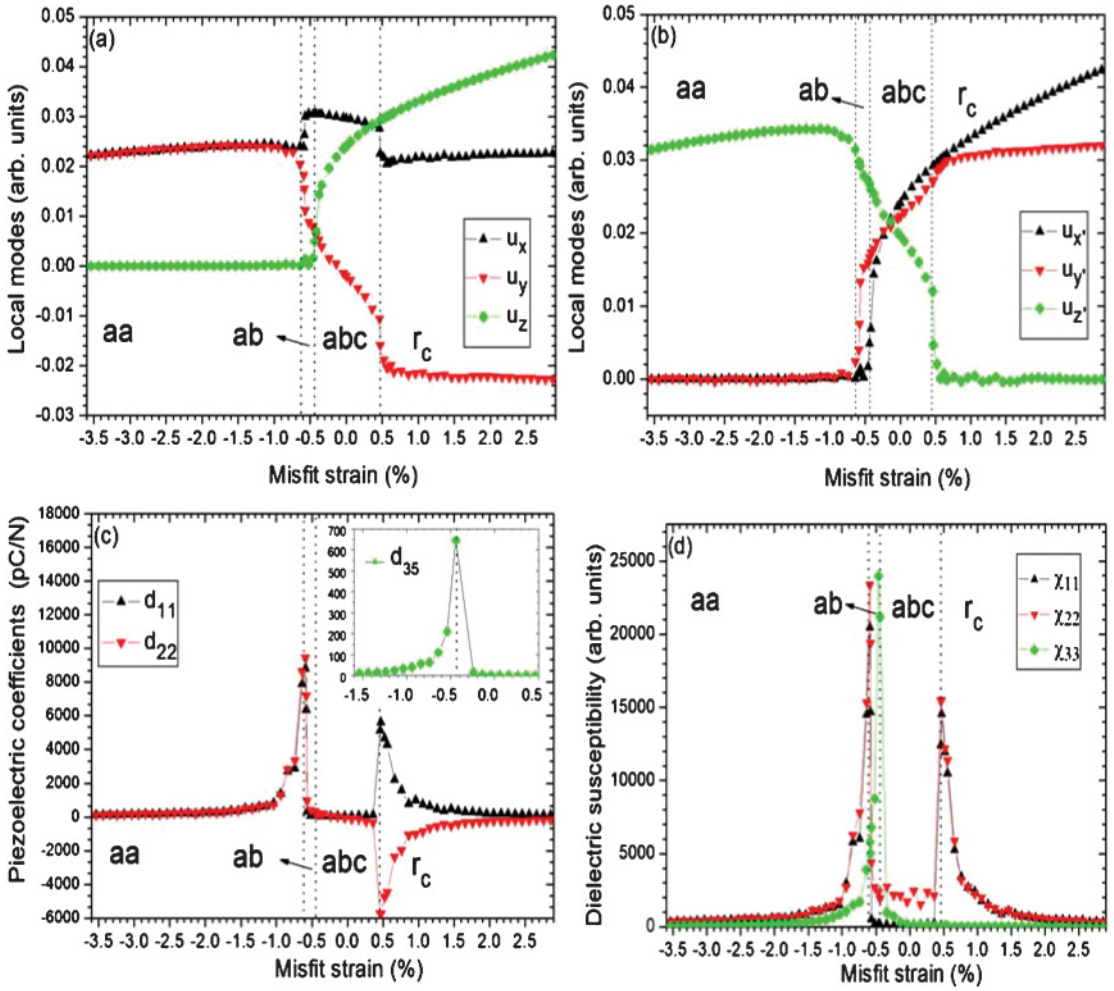

FIG. 3. (Color online) Strain dependency of properties in the (110) BTO film at 300 K. Panels (a) and (b): the local modes in the (xyz) and ($x'y'z'$) coordinate frame, respectively. Panels (c) and (d): the largest piezoelectric and dielectric coefficients, respectively—with the notation for subscript referring to the (xyz) frame.

As revealed by, e.g., comparing Fig. 1 and the results of Ref. 4, another major difference between (001) and (110) BTO films is the existence of the monoclinic ab and triclinic abc phases in these latter systems with a polarization lying along low-in-symmetry $[uw0]$ and $[uwv]$ directions, respectively. Such phases occur in a range of strain centered around 0.0% for temperature varying between 285 and 385 K and therefore exist at/near room temperature. Furthermore, Fig. 3 display the 300 K strain-dependency of the components of the local mode in the (xyz) and ($x'y'z'$) coordinate systems and of some components of the piezoelectric and dielectric tensors. u_y considerably changes with strain in the ab state, resulting in a polarization rapidly rotating from the out-of-plane [110] direction to [100] (that contains both in-plane and out-of-plane components), as δ varies between -0.6% and -0.4%. At this latter strain, the (110) BTO film acquires a z-component of the polarization, undergoing a phase transition towards the abc phase. Within this triclinic state, the y- and z-components of the polarization rapidly vary with the epitaxial strain. In particular, for a misfit strain around 0.0%, u_y passes through zero. The abc state then transforms into r_c via a transition that annihilates the out-of-plane component of the polarization. Figures 3(c) and 3(d) reveal that the polarization rotation occurring along the $aa \rightarrow ab \rightarrow abc \rightarrow r_c$ transition sequence generates huge dielectric and piezoelectric responses, especially in the vicinity of the aa-to-ab and ab-to-abc transitions, as consistent with the large responses found in the monoclinic and triclinic phases in $Pb(Zr,Ti)O_3$ systems under an electric field.[38] The strains needed to induce these aa-to-ab and ab-to-abc transitions in (110) BTO films are rather small, which is promising for the desired development of efficient (miniaturized) lead-free devices.[39] Another feature of Fig. 3(c) is also worth mentioning: the d_{22} piezoelectric coefficient changes its sign when δ goes from the compressive to the tensile strain region (as analogous to the corresponding change of the sign of u_y), which may be useful for some particular applications.[40,41]

IV. SUMMARY

In summary we have employed first-principles-based effective Hamiltonian approach[19,20] to mimic the finite-temperature properties of epitaxially grown (110) BTO films. BTO films grown along this particular direction exhibit a significantly different phase diagram from that of (001) BTO films. Examples of new features include: (i) the occurrence of phases occurring

in the tensile (respectively, compressive) strain region in (110) BTO films, while they appear in the compressive (respectively, tensile) region in the "normal" (001) BTO films; (ii) the discovery of novel monoclinic and triclinic phases [such phases do not exist in (001) films]; (iii) these monoclinic and triclinic phases have giant piezoelectric responses (around 10 000 pC/N, see Fig. 3) and phenomenal dielectric responses (over 20 000, see Fig. 3) at room temperature; (iv) the Curie temperature is independent of the strain in the compressive strain region, unlike in (001) BTO films, and this independency arises from the annihilation of various energetic terms; and (v) one can easily switch between different polarized states by applying in-plane and out-of-plane electric fields.

ACKNOWLEDGMENTS

We thank Jorge Iniguez, Wei Ren, and Yurong Yang for useful discussions. We mostly acknowledge ONR Grant Nos. N00014-11-1-0384 and N00014-08-1-0915 for financial support. NSF Grant Nos. DMR1066158 and DMR-0701558 and the Department of Energy, Office of Basic Energy Sciences, under contract ER-46612 are also acknowledged for discussions with scientists sponsored by these grants. Some computations were also made possible thanks to the MRI Grant No. 0959124 from NSF, N00014-07-1-0825 (DURIP) from ONR, and a Challenge Grant from HPCMO of the US Department of Defense.

*Corresponding author:zgui@uark.edu

[1] J. F. Scott, Annu. Rev. Mater. Sci. **28**, 79 (1998).
[2] D. Dimos and C. H. Mueller, Annu. Rev. Mater. Sci. **28**, 397 (1998).
[3] S. Bin-Omran, I. Ponomareva, and L. Bellaiche, Phys. Rev. B **77**, 144105 (2008).
[4] B.-K. Lai, I. Kornev, L. Bellaiche, and G. Salamo, Appl. Phys. Lett. **86**, 132904 (2005).
[5] O. Dieguez, S. Tinte, A. Antons, C. Bungaro, J. B. Neaton, K. M. Rabe, and D. Vanderbilt, Phys. Rev. B **69**, 212101 (2004).
[6] N. A. Pertsev, A. G. Zembilgotov, and A. K. Tagantsev, Phys. Rev. Lett. **80**, 1988 (1998).
[7] C. H. Ahn, K. M. Rabe, and J.-M. Triscone, Science **303**, 488 (2004).
[8] Y. Yoneda, T. Okabe, K. Sakaue, and H. Terauchi, Appl. Phys. **83**, 2458 (1998).
[9] I. B. Misirlioglu, S. P. Alpay, F. He, and B. O. Wells, J. Appl. Phys. **99**, 104103 (2006).
[10] J. H. Haeni, P. Irvin, W. Chang, R. Uecker, P. Reiche, Y. L. Li, S. Choudhury, W. Tian, M. E. Hawley, B. Craigo, A. K. Tagantsev, X. Q. Pan, S. K. Streiffer, L. Q. Chen, S. W. Kirchoefer, J. Levy, and D. G. Schlom, Nature (London) **430**, 758 (2004).
[11] N. A. Pertsev, A. K. Tagantsev, and N. Setter, Phys. Rev. B **61**, 825(R) (2000).
[12] I. Ponomareva and L. Bellaiche, Phys. Rev. B **74**, 064102 (2006).
[13] R. Oja, K. Johnston, J. Frantti, and R. M. Nieminen, Phys. Rev. B **78**, 094102 (2008).
[14] K. Sone, H. Naganuma, T. Miyazaki, T. Nakajima, and S. Okamura, Jpn. J. Appl. Phys. **49**, 09MB03 (2010).
[15] W. K. Simon, E. K. Akdogan, and A. Safari, J. Appl. Phys. **97**, 103530 (2005).
[16] W. K. Simon, E. K. Akdogan, A. Safari, and J. A. Bellotti, Appl. Phys. Lett. **87**, 082906 (2005); **88**, 132902 (2006).
[17] G. Akcay, I. B. Misirlioglu, and S. P. Alpay, Appl. Phys. Lett. **89**, 042903 (2006).
[18] S. Prosandeev, Igor A. Kornev, and L. Bellaiche, Phys. Rev. Lett. **107**, 117602 (2011).
[19] W. Zhong, D. Vanderbilt, and K. M. Rabe, Phys. Rev. Lett. **73**, 1861 (1994); Phys. Rev. B **52**, 6301 (1995).
[20] L. Walizer, S. Lisenkov, and L. Bellaiche, Phys. Rev. B **73**, 144105 (2006).
[21] A. García and D. Vanderbilt, Appl. Phys. Lett. **72**, 2981 (1998).
[22] K. M. Rabe and E. Cockayne, in *First-Principles Calculations for Ferroelectrics: Fifth Williamsburg Workshop*, edited by R. E. Cohen (AIP, Woodbury, New York, 1998), p. 61.
[23] S. Lisenkov and L. Bellaiche, Phys. Rev. B **76**, 020102(R) (2007).
[24] Q. Zhang and I. Ponomareva, Phys. Rev. Lett. **105**, 147602 (2010).
[25] S. Lisenkov and I. Ponomareva, Phys. Rev. B. **80**, 140102(R) (2009).
[26] J. Hlinka, T. Ostapchuk, D. Nuzhnyy, J. Petzelt, P. Kuzel, C. Kadlec, P. Vanek, I. Ponomareva, and L. Bellaiche, Phys. Rev. Lett. **101**, 167402 (2008).
[27] I. Ponomareva, L. Bellaiche, T. Ostapchuk, J. Hlinka, and J. Petzelt, Phys. Rev. B **77**, 012102 (2008).
[28] N. Choudhury, L. Walizer, S. Lisenkov, and L. Bellaiche, Nature (London) **470**, 513 (2011).
[29] N.A. Pertsev, V. G. Kukhar, H. Kohlstedt, and R. Waser, Phys. Rev. B **67**, 054107 (2003).
[30] D. Sichuga, I. Ponomareva, and L. Bellaiche, Phys. Rev. B **80**, 134116 (2009).
[31] See [http://stokes.byu.edu/findsym.html].
[32] The space group for the predicted phases in (110) BTO films is as follows. *p* state: orthorhombic *Cmmm*; *aa* state: orthorhombic *Amm*2; *c* state: orthorhombic *Cmm*2; *ab* state: monoclinic *Pm*; *abc* state: triclinic *P*1; r_{aa} state: monoclinic *Cm*; r_c state: monoclinic *Cm*.
[33] K. J. Choi, M. Biegalski, Y. L. Li, A. Sharan, J. Schubert, R. Uecker, P. Reiche, Y. B. Chen, X. Q. Pan, V. Gopalan, L.-Q. Chen, D. G. Schlom, and C. B. Eom, Science **306**, 1005 (2004).
[34] A. D. Bruce, Adv. Phys. **29**, 111 (1980).
[35] J. Íñiguez and L. Bellaiche, Phys. Rev. Lett **87**, 095503 (2001).
[36] P. Hohenberg and W. Kohn, Phys. Rev. **136**, 864 (1964); W. Kohn and L. J. Sham, *ibid.* **140**, A1133 (1965); G. Kresse and J. Hafner, Phys. Rev. B **47**, 558 (1993); G. Kresse and J. Furthmuller, *ibid.* **54**, 11169 (1996).
[37] Direct density-functional theory[36] calculations were carried out using the Vienna *ab initio* simulation package (VASP),[36] within local density approximation plus projector augmented-wave (PAW) method. 500-eV plane-wave cutoff energy is used as well as a 6 × 6 × 6 k-point grid.
[38] L. Bellaiche, A. García, and D. Vanderbilt, Phys. Rev. B **64**, 060103 (2001).
[39] Y. Guo, K.-I. Kakimoto, and H. Ohsato, Appl. Phys. Lett. **85**, 4121 (2004).
[40] D. Damjanovic, T. R. Gururaja, and L. E. Cross, Am. Ceram. Soc. Bull. **66**, 699 (1987).
[41] D. Damjanovic, T. R. Gururaja, S. J. Jang, and L. E. Cross, Mater. Lett. **4**, 414 (1986).